Available at
www.ElsevierComputerScience.com
POWERED BY SCIENCE DIRECT
Signal Processing 84 (2004) 2081–2096
SIGNAL PROCESSING
www.elsevier.com/locate/sigpro

A sequential Monte Carlo technique for blind synchronization and detection in frequency-flat Rayleigh fading wireless channels

Joaquín Míguez[a,*], Tadesse Ghirmai[b], Mónica F. Bugallo[b], Petar M. Djurić[b]

[a]Departamento de Electrónica e Sistemas, Universidade da Coruña, Campus de Elviña s/n, 15071 A Coruña, Spain
[b]Department of Electrical and Computer Engineering, Stony Brook University, Stony Brook, NY 11794, USA

Received 8 December 2003; received in revised form 22 April 2004

Abstract

This paper is aimed at the derivation of adaptive signal processing algorithms that jointly perform the tasks of blind data detection and generalized synchronization in a digital receiver. Optimal recovery of the synchronization parameters (timing, phase and frequency offsets) is analytically intractable and, as a consequence, most existing synchronization methods are either heuristic or based on approximate maximum likelihood (ML) arguments. We herein introduce an alternative approach derived within a Bayesian estimation framework and implemented via the sequential Monte Carlo (SMC) methodology. The algorithm is derived by considering an extended dynamic system where the reference parameters and the transmitted symbols are system-state random processes. The proposed model is well suited to represent frequency-flat fast-fading wireless channels. We also suggest two possible configurations for the receiver architecture that, combined with the proposed SMC technique, guarantee the achievement of asymptotically minimal symbol error rate (SER). The performance of the proposed technique is studied both analytically, by deriving the posterior Cramér–Rao bound (PCRB) for timing estimation, and through computer simulations that illustrate the accuracy of synchronization and the overall performance of the resulting blind receiver in terms of its SER.

Keywords: Synchronization; Monte Carlo; Particle filtering; Blind receivers

1. Introduction

Narrow band mobile communication links are generally modeled as frequency-flat Rayleigh fading channels. Recently, a lot of research work has been focused on the detection of signals over such channels [5,15,22]. However, most of these

*Corresponding author. Fax: +34-981-167160.
E-mail addresses: jmiguez@udc.es (J. Míguez), tadesse@ece.sunysb.edu (Tadesse. Ghirmai), monica@ece.sunysb.edu (M.F. Bugallo), djuric@ece.sunysb.edu (P.M. Djurić).

0165-1684/$ - see front matter
doi:10.1016/j.sigpro.2004.07.018

Nomenclature

s_m	mth transmitted symbol
$\mathcal{S}$	symbol alphabet
M	frame length
ω_k	discrete-time frequency offset process
a	roll-off factor
T_s	sampling period
y_k	discrete-time received signal
v_k	discrete-time noise signal
h_k	discrete-time complex amplitude of the received signal
τ_k	symbol delay at time k
L	inter-symbol interference (ISI) span
α	coefficient of the autoregressive process for the symbol timing
β_1, β_2	coefficients of the autoregressive process for the complex amplitude
γ	coefficient of the autoregressive process for the frequency offset
N	total number of particles
$(\mathbf{s}_{0:k}, \tau_{0:k}, \omega_{0:k})^{(n)}$	nth particle at time k
$w_k^{(n)}$	weight associated to the nth particle at time k
$p(\cdot)$	probability density function
$\pi(\cdot)$	importance (or proposal) probability density function
D	smoothing lag
$\mathbf{h}_k = [h_k, h_{k-1}]^\top$	channel vector
$\boldsymbol{\mu}_k$	channel mean at time k
$\boldsymbol{\Sigma}_k$	channel covariance at time k

contributions assume a perfect knowledge of the so-called synchronization parameters. It is broadly recognized that many practical communication channels present a high degree of structure and they can be accurately characterized through a set of reference parameters with a clear physical meaning. Since the observed signals collected by the receiver are affected by these parameters, they should be estimated, and compensated for, prior to data detection in order to achieve optimal or close-to-optimal performance. The generalized synchronization problem consists of the recovery of a set of such physical parameters as the symbol timing, phase offset and carrier frequency error. Unfortunately, optimal estimators of the parameters of interest cannot be derived in closed form and practical methods found in the literature [14,19] are either heuristic or based on approximate maximum likelihood (ML) arguments.

Sequential Monte Carlo (SMC) techniques [8,10] (also referred to as *particle filtering* methods) are powerful tools for Bayesian estimation that employ discrete measures with random support for representing posterior probability distributions of unknowns of interest. Recently, particle filtering has been successfully applied in digital communication problems, including applications such as channel estimation, equalization or space–time decoding (see [7] for a recent review of the subject). The SMC approach is also potentially useful for joint symbol detection and synchronization because it provides a way to numerically compute optimal Bayesian estimators when exact solutions cannot be derived analytically.

In order to apply common SMC algorithms, e.g., sequential importance sampling (SIS) [10], the only (and mild) requirement is that the observed signals can be written as a dynamic system in state-space form, which is usually simple to achieve with most communication signals. Existing SMC-based schemes which involve timing recovery and phase offset correction can be found in [2,3,12,16–18]. In [2,3] a pilot-data aided particle filtering algorithm is used for the estimation of the delay and the channel complex amplitude (which includes the phase offset) in a system with direct sequence spread spectrum (DSSS) modulation. A similar problem is addressed in [12], where the code-delay and the complex channel is estimated using a suboptimal (but complexity-restrained) combination of SMC methods and extended Kalman filtering, together with linear data detection. The problem of joint timing recovery, phase correction and data detection in DSSS modulated systems is addressed in [16–18] using particle filtering tools. In particular, a SMC algorithm based on deterministic sampling is presented and numerically evaluated in [18].

In this paper, we consider the problem of joint detection and non-data-aided generalized synchronization in general linearly modulated transmission systems using particle filtering. Specifically, we propose a new method for jointly and adaptively estimating the physical channel parameters (symbol timing, phase offset, channel amplitude and frequency error) and the transmitted data sequence, without the aid of any pilot symbols or training sequences. The SMC algorithm at the core of the new receiver is derived by considering an extended dynamic system where the symbol delay and the frequency error are modeled as first-order autoregressive (AR) stochastic processes [11] and the fading process of the complex channel (amplitude and phase) is modeled as a second-order AR process driven by complex white Gaussian noise [15]. The transmitted symbols are assumed independent and identically distributed (i.i.d.) random variables with a discrete uniform distribution. Within this framework we suggest two possible configurations to build an adequate receiver architecture that allows for complete removal of inter-symbol interference (ISI) and attains close-to-optimal symbol error rate (SER):

- An *open-loop* structure consisting of two branches, where the first one processes the received signal in order to compute frequency error, delay and complex channel estimates which are used in the second branch to sample the received signal with corrected timing epochs and adequately rotate the resulting observation to compensate the phase and frequency offsets.
- A *closed-loop* scheme that exploits the sequential structure of the proposed SMC algorithm to adaptively adjust the receiver timing, phase offset and frequency error estimates.

In both cases, symbol estimates can be obtained either directly from the particle filter or from the receiver matched filter after convergence of the synchronization parameter estimates.

The proposed receiver performance is assessed both analytically, by deriving the posterior Cramér–Rao bound (PCRB) for timing estimation, and through computer simulations. The latter allow to illustrate both the comparison of the delay estimates with the PCRB and the overall performance of the receiver in terms of its SER.

The remaining of the paper is organized as follows. Section 2 describes the signal model. The proposed SMC algorithm and the suggested receiver architectures are introduced in Sections 3 and 4, respectively. In Section 5, we proceed with an analytical study of the PCRB for timing estimation. Computer simulation results are presented in Section 6 and, finally, brief concluding remarks are made in Section 7.

2. Signal model

2.1. Received signal

Let us consider a digital communication system where symbols from a discrete alphabet, $s_m \in \mathcal{S}$, are transmitted in frames of length M. The baseband-equivalent received signal has the form

$$\tilde{y}(t) = h(t)e^{j\omega(t)t} \sum_{m=0}^{M-1} s_m \tilde{g}(t - mT + \tau(t)) + \tilde{v}(t) \quad (1)$$

where $h(t)$ is the complex multiplicative noise introduced by the frequency-flat Rayleigh fading channel, $\omega(t)$ is the carrier frequency error, s_m is the mth transmitted symbol, $\tilde{g}(t)$ is a squared-root raised-cosine pulse waveform, T is the symbol period, $0 \leqslant \tau(t) < T$ is the time-varying relative delay between the received signal and the local clock reference, and $\tilde{v}(t)$ is additive white Gaussian noise (AWGN) with power spectral density $N_0/2$. The receiver front-end consists of a matched filter that produces the signal

$$y(t) = h(t)e^{j\omega(t)t} \sum_{m=0}^{M-1} s_m g(t - mT + \tau(t)) + v(t) \quad (2)$$

where

$$g(t) = \tilde{g}(t) * \tilde{g}^*(-t) = \frac{\sin(\pi t/T)}{\pi t/T} \frac{\cos(\pi a t/T)}{1 - 4a^2t^2/T^2} \quad (3)$$

is a raised cosine waveform with roll-off factor $0 < a \leqslant 1$ and

$$v(t) = \int_{-\infty}^{\infty} \tilde{v}(u)\tilde{g}^*(u - t)\,\mathrm{d}u$$

is a Gaussian noise process with autocorrelation function $R_v(t) = (N_0/2)\,g(t)$.

Sampling the matched filter output with rate $1/T_s$ results in the discrete-time signal

$$y_k = h_k e^{j\omega_k k T_s} \sum_{m=0}^{M-1} s_m g(kT_s - mT + \tau_k) + v_k$$

where $y_k = y(kT_s)$, $h_k = h(kT_s)$, $\tau_k = \tau(kT_s)$, $\omega_k = \omega(kT_s)$, $v_k = v(kT_s)$, $k = 0, 1, 2, \dots$ is a discrete-time index and T_s is the sampling period.

Assuming that the raised cosine waveform, $g(t)$, has finite duration (which is always the case in practice) and symbol rate sampling, i.e., $T_s = T$, the previous expression can be rewritten as

$$y_k = h_k e^{j\omega_k k T} \sum_{n=1-L}^{L} s_{k+n} g(-nT + \tau_k) + v_k \tag{4}$$

where the fixed parameter L indicates the ISI span resulting from the limited time duration of $g(t)$. Note that, sampling at the symbol rate, the noise term $v_k = v(kT)$ remains white with variance $\sigma_v^2 = N_0/2$. Using vector notation, we arrive at the convenient representation

$$y_k = h_k e^{j\omega_k k T} \mathbf{g}(\tau_k)^\top \mathbf{s}_k + v_k \tag{5}$$

by defining the $2L \times 1$ channel vector

$$\mathbf{g}(\tau_k) = [g((L-1)T + \tau_k), g((L-2)T + \tau_k), \dots, g(-LT + \tau_k)]^\top \tag{6}$$

the symbol vector $\mathbf{s}_k = [s_{k-L+1}, s_{k-L+2}, \dots, s_{k+L}]^\top$ and using superindex $\top$ to denote transposition.

The general objective is to jointly and adaptively estimate the transmitted symbols, s_k, the signal timing, τ_k, the frequency error, ω_k, and the complex fading coefficients, h_k (which include both amplitude attenuation and phase offset), using the set of received signals, y_k, with $k = 0, \dots, M-1$.

2.2. State-space representation

The application of SMC techniques requires that the signals of interest be modeled as a dynamic system in state-space form. Following [11], we model the symbol timing as a first-order AR process,

$$\tau_k = \alpha\tau_{k-1} + u_k \tag{7}$$

where the perturbation variable, u_k, is assumed to be a zero-mean Gaussian with variance σ_u^2. Similarly, the variation of the frequency error is also modeled to follow a first-order AR process,

$$\omega_k = \gamma\omega_{k-1} + f_k \tag{8}$$

where f_k is a zero-mean white Gaussian process with variance σ_f^2. The dynamics of the fading coefficient, h_k, are adequately approximated using a second order AR model driven by complex white Gaussian noise, [15],

$$h_k = \beta_1 h_{k-1} + \beta_2 h_{k-2} + e_k \tag{9}$$

where the values of the coefficients of the autoregressive process, β_1 and β_2, and the variance of the zero-mean complex white Gaussian noise $e_k \sim \mathcal{N}(0, \sigma_e^2)$ are functions of the fading rate of the channel.

Taking into account the structure of $\mathbf{s}_k$, and combining (5), (7)–(9), we obtain the following dynamic state-space representation of the communication system:

$$\left.\begin{aligned} \tau_k &= \alpha\tau_{k-1} + u_k \\ \omega_k &= \gamma\omega_{k-1} + f_k \\ \mathbf{h}_k &= \mathbf{A}\mathbf{h}_{k-1} + \mathbf{c}e_k \\ \mathbf{s}_k &= \mathbf{S}\mathbf{s}_{k-1} + \mathbf{d}_k \end{aligned}\right\} \quad \text{state equation} \tag{10}$$

$$\left. y_k = e^{jkT\omega_k} \mathbf{c}^\top \mathbf{h}_k \mathbf{s}_k^\top \mathbf{g}(\tau_k) + v_k \right\} \quad \text{observation equation} \tag{11}$$

where

$$\mathbf{A} = \begin{bmatrix} \beta_1 & \beta_2 \\ 1 & 0 \end{bmatrix}$$

$\mathbf{h}_k = [h_k, h_{k-1}]^\top$, $\mathbf{c} = [1, 0]^\top$,

$$\mathbf{S} = \begin{bmatrix} 0 & 1 & 0 & \cdots & 0 \\ 0 & 0 & 1 & \cdots & 0 \\ \vdots & \vdots & \vdots & \ddots & \vdots \\ 0 & 0 & 0 & \cdots & 1 \\ 0 & 0 & 0 & \cdots & 0 \end{bmatrix}$$

is an $2L \times 2L$ shifting matrix, $\mathbf{s}_k = [s_{k-L+1}, \dots, s_{k+L}]^\top$ is an $2L \times 1$ vector, and $\mathbf{d}_k = [0, \dots, 0, s_{k+L}]^\top$ is a $2L \times 1$ perturbation vector that contains the new symbol, s_{k+L}. Note that the system state at time k is given by $(\mathbf{s}_k, \mathbf{h}_k, \tau_k, \omega_k)$, while the model parameters, α, σ_u^2, γ, σ_f^2, β_1, β_2, σ_e^2, σ_v^2 and L, are assumed fixed and known.

2.3. Validity of the model

The choice of AR process for the modeling of the synchronization and channel parameters of interest is due both to mathematical tractability and the flexibility of this class of random process to faithfully approximate the statistical characteristics of more complicated models.

Indeed, the use of AR processes to represent the complex fading of typical wireless channels has been proposed and adequately justified in several papers (see [15,13] for a recent discussion). It is usually accepted that a second-order AR process is sufficient to sensibly approximate the dynamics of most statistical wireless-channel models [13], which are normally specified in terms of their second-order statistics. The AR parameters (β_i, σ_e^2) are easily chosen to match the autocorrelation function of the desired channel model using the Yule–Walker equations.

AR modeling of the symbol delay was suggested in [11], and we follow the same approach here both for τ_k and the frequency error ω_k. Unfortunately, the statistical representation of the fluctuations in these magnitudes due to highly dynamic environments (such as those encountered by communication terminals in high speed vehicles) is not as well studied as that of fading. We note, however, that the same approach of choosing the AR model order and parameters to match the statistics of any other model available (including ad hoc models obtained from specific field measurements) is straightforward. It is likely that, in a practical situation, an AR process with order higher than 1 is needed, but this can be handled easily in the same way as it is done with the fading coefficients in this paper.

Finally, the variance of the AWGN in the observation equation (4) can be either a priori set, given the signal-to-noise ratio (SNR) region where the transmission system is expected to operate, or, alternatively, it can be estimated prior to synchronization and detection.

3. A sequential Monte Carlo method for joint synchronization and data detection

In this section, we propose an efficient particle filtering algorithm for joint reference parameters estimation and data detection. We focus on the joint estimation of the symbols, $s_{0:M-1} = \{s_0, \ldots, s_{M-1}\}$, the delays, $\tau_{0:M-1} = \{\tau_0, \ldots, \tau_{M-1}\}$, and the frequency error, $\omega_{0:M-1} = \{\omega_0, \ldots, \omega_{M-1}\}$, from the available observations, $y_{0:M-1} = \{y_0, \ldots, y_{M-1}\}$. The complex fading process $h_{0:M-1} = \{h_0, \ldots, h_{M-1}\}$ is handled as a *nuisance* process which is analytically integrated out. Nevertheless, estimates of h_k can be easily computed when necessary, as will be shown in Section 4.

3.1. Particle filtering

We are interested in the sequential estimation of the transmitted data, symbol timing and frequency error. From a Bayesian perspective, all necessary information is contained in the joint posterior probability distribution function (pdf), $p(\mathbf{s}_{0:k}, \tau_{0:k}, \omega_{0:k} \mid y_{0:k})$. Unfortunately, the latter distribution is analytically intractable and prevents the derivation of closed-form Bayesian estimators. An emerging, powerful signal processing tool suitable to deal with such a problem is *particle filtering*. *Particle filters* consist of discrete measures with random support that approximate desired posterior pdfs and can be sequentially updated. Specifically, we denote the discrete measure at time k by

$$\Xi_k = \{(\mathbf{s}_{0:k}, \tau_{0:k}, \omega_{0:k})^{(n)}, w_k^{(n)}\}_{n=1}^N \tag{12}$$

where $\mathbf{s}_{0:k}^{(n)}$, $\tau_{0:k}^{(n)}$, and $\omega_{0:k}^{(n)}$ are sample trajectories of the data, the delay and the frequency error processes, respectively, and they are usually referred to as *particles*, while $w_k^{(n)}$ are *weights* that approximate the posterior probability of the nth particle, $(\mathbf{s}_{0:k}, \tau_{0:k}, \omega_{0:k})^{(n)}$. Note that, in trivial applications where sampling directly from the desired distribution is feasible, the weights are all equal, $w_k^{(n)} = 1/N \quad \forall n$.

Using (12), it can be shown [6] that the posterior pdf approximated as

$$\hat{p}(\mathbf{s}_{0:k}, \tau_{0:k}, \omega_{0:k}|y_{0:k}) = \sum_{n=1}^{N} w_k^{(n)} \delta((\mathbf{s}_{0:k}, \tau_{0:k}, \omega_{0:k}) - (\mathbf{s}_{0:k}, \tau_{0:k}, \omega_{0:k})^{(n)}) \quad (13)$$

where $\delta(\cdot)$ is Dirac's delta function, converges in mean squared error to $p(\mathbf{s}_{0:k}, \tau_{0:k}, \omega_{0:k}|y_{0:k})$ as $N \to \infty$.

Bayesian estimators of the data, the delay, the frequency error, or all of them jointly, are straightforward to derive using the approximated posterior pdf. For instance, if we work with the minimum mean square error (MMSE) estimator of the delay, we have

$$\hat{\tau}_{0:k}^{\text{mmse}} = \sum_{n=1}^{N} w_k^{(n)} \tau_{0:k}^{(n)}. \quad (14)$$

Similarly, the MMSE estimator of the frequency offset is,

$$\hat{\omega}_{0:k}^{\text{mmse}} = \sum_{n=1}^{N} w_k^{(n)} \omega_{0:k}^{(n)} \quad (15)$$

and the maximum a posteriori (MAP) estimate of the data sequence is[1]

$$\hat{\mathbf{s}}_{0:k}^{\text{map}} = \arg\max_{\mathbf{s}_{0:k}} \left\{ \sum_{n=1}^{N} w_k^{(n)} \delta((\mathbf{s}_{0:k}, \tau_{0:k}, \omega_{0:k}) - (\mathbf{s}_{0:k}, \tau_{0:k}, \omega_{0:k})^{(n)}) \right\}. \quad (16)$$

3.2. Sequential importance sampling

A major advantage of the particle filtering approach is the possibility to build the discrete measure Ξ_k sequentially, i.e., to compute Ξ_k recursively from Ξ_{k-1} once the kth observation, y_k, becomes available. Algorithms for the recursive computation of discrete measures are usually termed SMC methods [9]. One of the most popular SMC techniques is the so-called SIS algorithm [10].

According to the IS principle [9], an empirical approximation of a desired pdf, $p(x)$, can be obtained by drawing particles from an *importance function* or *proposal pdf*, $\pi(x)$, which

- is strictly positive, $\pi(x) > 0$,
- has the same domain as $p(x)$, and
- is easy to sample from.

The resulting particles, $x^{(n)} \sim \pi(x)$, are assigned (unnormalized) weights of the form

$$\tilde{w}^{(n)} = \frac{p(x^{(n)})}{\pi(x^{(n)})} \quad (17)$$

which are said to be *proper*, meaning that

$$E_{\pi(x)}[x\tilde{w}] = E_{\pi(x)}\left[x\frac{p(x)}{\pi(x)}\right] = E_{p(x)}[x] \quad (18)$$

where $E_{p(x)}[\cdot]$ denotes expected value with respect to the pdf in the subscript. In the synchronization application presented in this paper, the desired distribution is $p(\mathbf{s}_{0:k}, \tau_{0:k}, \omega_{0:k}|y_{0:k})$, hence an importance function of the form $\pi(\mathbf{s}_{0:k}, \tau_{0:k}, \omega_{0:k}|y_{0:k})$ is needed.

The sequential application of the IS principle is possible by resorting to the recursive decomposition of the posterior distribution

$$\begin{aligned} p(\mathbf{s}_{0:k}, \tau_{0:k}, \omega_{0:k}|y_{0:k}) &\propto p(y_k|\mathbf{s}_{0:k}, \tau_{0:k}, \omega_{0:k}, y_{0:k-1}) \\ &\quad \times p(\mathbf{s}_{0:k}, \tau_{0:k}, \omega_{0:k}|y_{0:k-1}) \\ &\propto p(y_k|\mathbf{s}_{0:k}, \tau_{0:k}, \omega_{0:k}, y_{0:k-1}) \\ &\quad \times p(\tau_k|\tau_{k-1}) p(\omega_k|\omega_{k-1}) \\ &\quad \times p(\mathbf{s}_{0:k-1}, \tau_{0:k-1}, \\ &\quad \times \omega_{0:k-1}|y_{0:k-1}) \end{aligned} \quad (19)$$

which is easily derived using Bayes theorem and the a priori uniform probability distribution of the transmitted symbols. Assuming a proposal pdf that admits a factorization of the form

$$\begin{aligned} &\pi(\mathbf{s}_{0:k}, \tau_{0:k}, \omega_{0:k}|y_{0:k}) \\ &\quad = \pi(\mathbf{s}_k, \tau_k, \omega_k|\mathbf{s}_{0:k-1}, \tau_{0:k-1}, \omega_{0:k-1}, y_{0:k}) \\ &\qquad \times \pi(\mathbf{s}_{0:k-1}, \tau_{0:k-1}, \omega_{0:k-1}|y_{0:k-1}) \end{aligned} \quad (20)$$

Eq. (19) can be used to recursively compute the discrete measure at time k, Ξ_k, from Ξ_{k-1}

[1] Note that estimating $\mathbf{s}_{0:k}$ is equivalent to estimating $s_{0:k+L}$, since $\mathbf{s}_k = [s_{k-L+1}, \ldots, s_{k+L}]^\top$ and, for $k < 0$, we can assume $s_{k<0} = b$ where b is a known signal level.

and the new observation, y_k, by taking the following steps:

(1) Importance sampling:

$$(\mathbf{s}_k, \tau_k)^{(n)} \sim \pi(\mathbf{s}_k, \tau_k, \omega_k | \mathbf{s}_{0:k-1}^{(n)}, \tau_{0:k-1}^{(n)}, \omega_{0:k-1}^{(n)}, y_{0:k}) = \pi_k(s_{k+L}, \tau_k, \omega_k). \quad (21)$$

(2) Weight update:

$$\tilde{w}_k^{(n)} = w_{k-1}^{(n)} \frac{p(y_k | \mathbf{s}_{0:k}^{(n)}, \tau_{0:k}^{(n)}, \omega_{0:k}^{(n)}, y_{0:k-1}) p(\tau_k^{(n)} | \tau_{k-1}^{(n)}) p(\omega_k^{(n)} | \omega_{k-1}^{(n)})}{\pi_k(s_{k+L}^{(n)}, \tau_k^{(n)}, \omega_k^{(n)})}. \quad (22)$$

(3) Weight normalization:

$$w_k^{(n)} = \frac{\tilde{w}_k^{(n)}}{\sum_{i=1}^N \tilde{w}_k^{(i)}}. \quad (23)$$

3.3. Computation

The proposed SIS algorithm requires the numerical evaluation of the likelihood function in the weight update equation. Let $\mathcal{N}(\mathbf{x}; \boldsymbol{\mu}, \boldsymbol{\Sigma})$ denote the multivariate Gaussian distribution with mean $\boldsymbol{\mu}$ and covariance $\boldsymbol{\Sigma}$. It is straightforward to show that

$$p(y_k | \mathbf{s}_{0:k}, \tau_{0:k}, \omega_{0:k}, y_{0:k-1}) = \int_{\mathbf{h}_k} p(y_k | \mathbf{s}_k, \tau_k, \omega_k, \mathbf{h}_k) \times p(\mathbf{h}_k | \mathbf{s}_{0:k-1}, \tau_{0:k-1}, \omega_{0:k-1}, y_{0:k-1}) \, d\mathbf{h}_k \quad (24)$$

where

$$p(y_k | \mathbf{s}_k, \omega_k, \tau_k, \mathbf{h}_k) = \mathcal{N}(y_k; h_k e^{jkT\omega_k} \mathbf{g}^\top(\tau_k) \mathbf{s}_k, \sigma_v^2) \quad (25)$$

and

$$p(\mathbf{h}_k | \mathbf{s}_{0:k-1}, \tau_{0:k-1}, \omega_{0:k-1}, y_{0:k-1}) = \mathcal{N}(\mathbf{h}_k; \boldsymbol{\mu}_{k|k-1}, \boldsymbol{\Sigma}_{k|k-1}) \quad (26)$$

are complex Gaussian pdf's. Notice that the predictive channel mean,

$$\boldsymbol{\mu}_{k|k-1} = E_{p(\mathbf{h}_k | \mathbf{s}_{0:k-1}, \tau_{0:k-1}, \omega_{0:k-1}, y_{0:k-1})}[\mathbf{h}_k] \quad (27)$$

and the predictive covariance matrix,

$$\boldsymbol{\Sigma}_{k|k-1} = E_{p(\mathbf{h}_k | \mathbf{s}_{0:k-1}, \tau_{0:k-1}, \omega_{0:k-1}, y_{0:k-1})} \times [(\mathbf{h}_k - \boldsymbol{\mu}_{k|k-1})(\mathbf{h}_k - \boldsymbol{\mu}_{k|k-1})^H] \quad (28)$$

can be analytically computed using a Kalman filter. Therefore, the integral in (24) can be solved to yield

$$p(y_k | \mathbf{s}_{0:k}, \tau_{0:k}, \omega_{0:k}, y_{0:k-1}) = \mathcal{N}(y_k; \bar{y}_k, \sigma_{y_k}^2) \quad (29)$$

where

$$\bar{y}_k = e^{jkT\omega_k} \mathbf{g}(\tau_k)^\top \mathbf{s}_k \mathbf{c}^\top \boldsymbol{\mu}_{k|k-1} \quad (30)$$

and

$$\sigma_{y_k}^2 = \sigma_v^2 + (e^{jkT\omega_k} \mathbf{g}^\top(\tau_k) \mathbf{s}_k \mathbf{c}^\top) \boldsymbol{\Sigma}_{k|k-1} \times (e^{jkT\omega_k} \mathbf{g}^\top(\tau_k) \mathbf{s}_k \mathbf{c}^\top)^H. \quad (31)$$

As for the importance function, at time k we choose

$$\pi_k \quad (s_k, \tau_k, \omega_k) = p(s_{k+L} | \mathbf{s}_{0:k-1}^{(n)}, \tau_k, \omega_k, \tau_{0:k-1}^{(n)}, \omega_{0:k-1}^{(n)}, y_{0:k}) \times p(\tau_k | \tau_{k-1}^{(n)}) p(\omega_k | \omega_{k-1}^{(n)}) \quad (32)$$

which can be sampled in three steps. First, we obtain a new delay particle,

$$\tau_k^{(n)} \sim \mathcal{N}(\alpha \tau_{k-1}^{(n)}, \sigma_u^2). \quad (33)$$

Then, a sample of the frequency error,

$$\omega_k^{(n)} = \mathcal{N}(\gamma \omega_{k-1}^{(n)}, \sigma_f^2). \quad (34)$$

Finally, a sample of the transmitted symbol is drawn from the first density in the right-hand side of (32). This is feasible because we can rewrite $p(\mathbf{s}_k | \mathbf{s}_{0:k-1}^{(n)}, \tau_{0:k}^{(n)}, \omega_{0:k}^{(n)}, y_{0:k})$ as

$$p(s_{k+L} = S | \mathbf{s}_{0:k-1}^{(n)}, \tau_{0:k}^{(n)}, \omega_{0:k}^{(n)}, y_{0:k}) \propto p(y_k | s_{k+L} = S, \mathbf{s}_{0:k-1}^{(n)}, \tau_{0:k}^{(n)}, \omega_{0:k}^{(n)}, y_{0:k-1}) \quad (35)$$

where $S \in \mathcal{S}$ is a symbol in the modulation alphabet, $\mathcal{S}$. Notice that the likelihood in the right-hand side of (35) can be evaluated using (29). The resulting importance weights for the new particles are given by

$$w_k^{(n)} \propto w_{k-1}^{(n)} \sum_{S_j \in \mathcal{A}} \mathcal{N}(y_k; \bar{y}_k^{(n)}, \sigma_{y_k}^{2\ (n)}) \quad (36)$$

where

$$\bar{y}_k^{(n)} = e^{jkT\omega_k}\mathbf{g}^\top(\tau_k^{(n)})\mathbf{s}_{k,j}^{(n)}\mathbf{c}^\top\boldsymbol{\mu}_{k|k-1}^{(n)} \quad (37)$$

$$\sigma_{y_k}^{2,(n)} = \sigma_v^2 + (e^{jkT\omega_k}\mathbf{g}^\top(\tau_k^{(n)})\mathbf{s}_{k,j}^{(n)}\mathbf{c}^\top)\boldsymbol{\Sigma}_{k|k-1}^{(n)} \times(e^{jkT\omega_k}\mathbf{g}^\top(\tau_k^{(n)})\mathbf{s}_{k,j}^{(n)}\mathbf{c}^\top)^H \quad (38)$$

$\mathbf{s}_{k,j}^{(n)} = [s_{k-L+1}^{(n)}, \ldots, s_{k+L-1}^{(n)}, s_{k+L} = S_j]^\top$, and $\boldsymbol{\mu}_{k|k-1}^{(n)}$ and $\boldsymbol{\Sigma}_{k|k-1}^{(n)}$ are the predictive channel mean and covariance matrix, respectively, obtained by Kalman filtering from the observations and the nth state trajectory, $(\mathbf{s}_{0:k-1}, \tau_{0:k-1}, \omega_{0:k-1})^{(n)}$.

It is important to remark that the implementation of the proposed SIS algorithm requires a bank of Kalman filters (one for each particle) in order to compute the fading process statistics that are needed for the importance pdf and the weight update equation. The combination of the SIS algorithm and Kalman filtering is often termed mixture kalman filter (MKF), and it has both been applied to communications problems [5] and described as a general procedure to handle so-called conditionally-linear Gaussian systems [4,10].

3.4. Smoothing

An important characteristic of the digital transmission system represented by (11) is that, for $\tau_k > 0$, each transmitted symbol contributes to $2L$ successive observations, where L is the ISI span parameter. Specifically, the symbol s_k, is a component of each data vector in the sequence

$$\mathbf{s}_{k-L:k+L-1} = \{\mathbf{s}_{k-L}, \mathbf{s}_{k-L+1}, \ldots, \mathbf{s}_{k+L-1}\} \quad (39)$$

and, therefore, it is statistically dependent on the corresponding observations,

$$y_{k-L:k+L-1} = \{y_{k-L}, y_{k-L+1}, \ldots, y_{k+L-1}\}. \quad (40)$$

As a consequence, the reliable detection of the symbol sequence up to time k, $s_{0:k}$, requires the adequate processing of (at least) the observations $y_{0:k+L-1}$.

In order to account for the effect of ISI, it is convenient to estimate the transmitted data from the posterior distribution $p(\mathbf{s}_{0:k-D}, \tau_{0:k}, \omega_{0:k}|y_{0:k})$, where $D \leqslant L+1$ is a fixed smoothing lag (see, e.g., [7]). The SIS algorithm can still be used to recursively compute the particle filter for the smooth distribution,

$$\Delta_k = \left\{(\mathbf{s}_{0:k-D}, \tau_{0:k}, \omega_{0:k})^{(n)}, w_k^{(n)}\right\}_{n=1}^N. \quad (41)$$

In particular, the importance sampling and weight update Eqs. (21) and (22), respectively, are substituted by

$$(\mathbf{s}_{k-D}, \tau_k, \omega_k)^{(n)} \sim \pi(\mathbf{s}_{k-D}, \tau_k, \omega_k|\mathbf{s}_{0:k-D-1}^{(n)}, \tau_{0:k-1}^{(n)}, \omega_{0:k-1}^{(n)}, y_{0:k}) \quad (42)$$

and

$$\tilde{w}_k^{(n)} = w_{k-1}^{(n)} \frac{p(\tau_k^{(n)}|\tau_{k-1}^{(n)})p(\omega_k^{(n)}|\omega_{k-1}^{(n)})L_k^{(n)}(D)}{\pi(\mathbf{s}_{k-D}^{(n)}, \tau_k^{(n)}, \omega_k^{(n)}|\mathbf{s}_{0:k-D-1}^{(n)}, \tau_{0:k-1}^{(n)}, \omega_{0:k-1}^{(n)}, y_{0:k})} \quad (43)$$

where $L_k^{(n)}(D)$ is the smooth likelihood

$$L_k^{(n)}(D) = \sum_{\mathscr{S}^D} p(y_{k-D:k}|\mathbf{s}_{0:k-D}^{(n)}, s_{k-D+L+1:k+L}, \tau_{0:k}^{(n)}, \omega_{0:k}^{(n)}, y_{0:k-D-1}).$$

The summation $\sum_{\mathscr{S}^D}(\cdot)$ in the above equation is carried out over all possible combinations of the sequence $s_{k-D+L+1:k+L} \in \mathscr{S}^D$. Given the nth particle, $\mathbf{s}_{k-D}^{(n)}$, each symbol combination yields one sequence of subsequent data vectors, $\mathbf{s}_{k-D+1:k}$.

A convenient form of the proposal distribution in (42) is

$$\pi(\mathbf{s}_{k-D}, \tau_k, \omega_k|\mathbf{s}_{0:k-D-1}^{(n)}, \tau_{0:k-1}^{(n)}, \omega_{0:k-1}^{(n)}, y_{0:k}) = p(\tau_k|\tau_{k-1}^{(n)})p(\omega_k|\omega_{k-1}^{(n)})p(\mathbf{s}_{k-D}|\mathbf{s}_{0:k-D-1}^{(n)}, \tau_{0:k}^{(n)}, \omega_{0:k}^{(n)}, y_{0:k}) \quad (44)$$

which allows to sample particles in three steps. First, the delay is drawn as

$$\tau_k^{(n)} \sim \mathscr{N}(\alpha\tau_{k-1}^{(n)}, \sigma_u^2). \quad (45)$$

Then, a sample of the frequency offset is drawn from

$$\omega_k^{(n)} \sim \mathscr{N}(\gamma\omega_{k-1}^{(n)}, \sigma_f^2). \quad (46)$$

Finally, the vector $\mathbf{s}_{k-D}^{(n)}$ is sampled from $p(\mathbf{s}_{k-D}|\mathbf{s}_{0:k-D-1}^{(n)}, \tau_{0:k}^{(n)}, \omega_{0:k}^{(n)}, y_{0:k})$. Recalling that the symbols are modeled as i.i.d. uniform random variables, the latter distribution can be decomposed as

$$p(\mathbf{s}_{k-D}|\mathbf{s}_{0:k-D-1}^{(n)}, \tau_{0:k}^{(n)}, \omega_{0:k}^{(n)}, y_{0:k}) \propto \sum_{\mathscr{S}^D} p(y_{k-D:k}|\mathbf{s}_{k-D}, \mathbf{s}_{0:k-D-1}^{(n)}, s_{k-D+L+1:k+L}, \tau_{0:k}^{(n)}, \omega_{0:k}^{(n)}, y_{0:k-D-1}). \quad (47)$$

Notice that in order to build $\mathbf{s}_{k-D}^{(n)}$ given $\mathbf{s}_{k-D-1}^{(n)}$ only one symbol, s_{k-D+L}, needs to be sampled. Thus, we draw

$$s_{k-D+L}^{(n)} \sim \rho^{(n)}(s_{k-D+L}) \quad (48)$$

and let

$$\mathbf{s}_{k-D}^{(n)} = \mathbf{S}\mathbf{s}_{k-D-1}^{(n)} + [0, \ldots, 0, s_{k-D+L}^{(n)}]^\top. \quad (49)$$

The probability mass function (pmf) $\rho^{(n)}(s_{k-D+L})$ is defined according to (47), i.e.,

$$\rho^{(n)}(s_{k-D+L}) = \frac{\sum_{\mathscr{S}^D} p(y_{k-D:k}|\mathbf{s}_{0:k-D-1}^{(n)}, s_{k-D+L}, s_{k-D+L+1:k+L}, \tau_{0:k}^{(n)}, \omega_{0:k}^{(n)}, y_{0:k-D-1})}{\sum_{\mathscr{S}^{D+1}} p(y_{k-D:k}|\mathbf{s}_{0:k-D-1}^{(n)}, s_{k-D+L:k+L}, \tau_{0:k}^{(n)}, \omega_{0:k}^{(n)}, y_{0:k-D-1})}, \quad (50)$$

where the summation $\sum_{\mathscr{S}^{D+1}}(\cdot)$ is over all possible combinations of the sequence $s_{k-D+L:k+L} \in \mathscr{S}^{D+1}$ and the likelihoods can be computed as

$$p(y_{k-D:k}|\mathbf{s}_{0:k}, \tau_{0:k}, \omega_{0:k}^{(n)}, y_{0:k-D-1}) \propto \prod_{j=0}^{D} \mathscr{N}(y_{k-j}; \bar{y}_{k-j}, \sigma_{y_{k-j}}^2). \quad (51)$$

The latter equation means that, at time k, a Kalman smoother has to be run for each particle and for each possible combination of symbols $s_{k-D+L:k+L}$.

The particle filter Δ_k can be used to sequentially estimate the synchronization parameters and received data, namely

$$\hat{\tau}_k^{\text{mmse}} = \sum_{n=1}^{N} \tau_k^{(n)} w_k^{(n)} \quad (52)$$

$$\hat{\omega}_k^{\text{mmse}} = \sum_{n=1}^{N} \omega_k^{(n)} w_k^{(n)} \quad (53)$$

are MMSE estimates of the timing and frequency error, respectively, and

$$\hat{s}_{k-D}^{\text{map}} = \arg \max_{s_{k-D} \in \mathscr{S}} \left\{ \sum_{n=1}^{N} w_k^{(n)} \delta^{(n)}(s_{k-D}^{(n)} - s_{k-D}) \right\} \quad (54)$$

is the marginal MAP estimate of s_{k-D} given $y_{0:k}$.

3.5. Resampling

A major problem in the practical implementation of the SIS algorithm described so far is that the discrete measure, Δ_k, degenerates quickly, i.e., after a few time steps, most of the importance weights have negligible values ($w_k^{(n)} \simeq 0$) and only a few particles with significant weights remain *useful*. The common solution to this problem is to *resample* the particles [10]. Resampling is an algorithmic step that stochastically eliminates particles with small weights, while those with larger weights are replicated. In its simplest form, resampling takes Δ_k as an input and produces a new discrete measure $\tilde{\Delta}_k = \{(\tilde{\mathbf{s}}_{0:k-D}, \tilde{\tau}_{0:k}, \tilde{\omega}_{0:k})^{(n)}, \frac{1}{N}\}_{n=1}^{N}$, where $(\tilde{\mathbf{s}}_{0:k-D}^{(n)}, \tilde{\tau}_{0:k}^{(n)}, \tilde{\omega}_{0:k}^{(n)}) = (\mathbf{s}_{0:k-D}^{(i)}, \tau_{0:k}^{(i)}, \omega_{0:k}^{(i)})$ with probability $w_k^{(i)}$.

4. Receiver architecture

Although the transmitted data with their timing can be estimated together using the SIS algorithm described above, it is important to notice that the proposed method does not remove the ISI. In other words, although the relative symbol delays, τ_k, are estimated, the sampling instants, $t = kT$, are not corrected to attain a better timing and avoid ISI. As a consequence, the SER that can be attained by detecting according to (54) is lower bounded by the SER of the maximum likelihood sequence detector (MLSD) with perfect knowledge of the sequence of channel vectors $e^{jkT\omega_k} h_k \mathbf{g}(\tau_k)$. In general, and assuming the autocorrelation function of the continuous-time synchronization processes, ($\tau(t)$, $\omega(t)$ and $h(t)$) is wider than the symbol period, a lower SER is achieved with a matched-filter receiver sampled at $t = kT - \hat{\tau}_k$ (where $\hat{\tau}_k$is a delay estimate) because ISI-free observations can be obtained.

The SER of the matched detector can be attained with the proposed SMC algorithm if an adequate receiver architecture is used. In this section, we present two possible configurations that use the SMC approach for recovering the timing and removing ISI before detection.

4.1. Open-loop receiver

In the first place, we consider the double branch structure depicted in Fig. 1. In the upper branch, the SMC block performs the proposed SIS algorithm, which is used to compute Monte Carlo MMSE estimates of the timing according to (53). The received signal is held in the lower branch, until the delay estimate is computed, and then sampled at $t = kT - \hat{\tau}_k^{\mathrm{mmse}}$ to obtain the observation

$$\begin{aligned}\hat{y}_k &= y(kT - \hat{\tau}_k^{\mathrm{mmse}}) \\ &= \mathrm{e}^{j(kT-\hat{\tau}_k^{\mathrm{mmse}})\omega_k} h_k \mathbf{s}_k^\top \mathbf{g}(\tau_k - \hat{\tau}_k^{\mathrm{mmse}}) + v_k \end{aligned} \tag{55}$$

where $\mathbf{s}_k = [s_{k-L+1}, \ldots, s_{k+L}]^\top$, if $\tau_k - \hat{\tau}_k^{\mathrm{mmse}} > 0$, and $\mathbf{s}_k = [s_{k-L}, \ldots, s_{k+L-1}]^\top$, if $\tau_k - \hat{\tau}_k^{\mathrm{mmse}} < 0$. Note that, with the corrected epoch, $\omega_k = \omega(kT - \hat{\tau}_k^{\mathrm{mmse}})$, $\tau_k = \tau(kT - \hat{\tau}_k^{\mathrm{mmse}})$ and $h_k = h(kT - \hat{\tau}_k^{\mathrm{mmse}})$

Ideally, when $\hat{\tau}_k^{\mathrm{mmse}} \simeq \tau_k$, the ISI is removed and

$$\hat{y}_k \simeq \mathrm{e}^{j(kT-\hat{\tau}_k^{\mathrm{mmse}})\omega_k} h_k s_k + v_k, \tag{56}$$

hence minimal SER is achieved by and adequate de-rotation of $\hat{y}_k$, multiplying by $\mathrm{e}^{-j((kT-\hat{\tau}_k^{\mathrm{mmse}})\hat{\omega}_k^{\mathrm{mmse}}} \hat{h}_k^*$, followed by a simple threshold detector. The aforementioned channel estimate is computed as

$$\hat{h}_k = \sum_{n=1}^{N} \mathbf{c}^\top \boldsymbol{\mu}_k^{(n)} w_{k+D}^{(n)} \tag{57}$$

where

$$\boldsymbol{\mu}_k^{(n)} = \mathrm{E}_{p(\mathbf{h}_k | \mathbf{s}_{0:k}^{(n)}, \tau_{0:k}^{(n)}, \omega_{0:k}^{(n)}, y_{0:k})}[\mathbf{h}_k] \tag{58}$$

is the posterior channel estimate associated to the nth particle and calculated by Kalman filtering. Note, however, that this estimate cannot be obtained until the symbols up to time k, $\{\mathbf{s}_{0:k}^{(n)}\}_{n=1}^N$, are available in the particle filter, which occurs at time $k + D$ due to the smoothing. Hence there is need to hold $\hat{y}_k$ until it can be conveniently de-rotated for accurate detection, as depicted in Fig. 1.

The recursive steps of the proposed SMC algorithm with the open-loop architecture are summarized in Table 1.

4.2. Closed-loop receiver

The main drawback of the previous configuration is the fact that the received signal is sampled twice per symbol period. To avoid this drawback, the closed-loop receiver architecture shown in Fig. 2 can be used.

The SMC block represents the SIS algorithm with resampling described in Section 3, which yields asymptotically optimal MMSE estimates of the relative symbol delay, $\hat{\tau}_k^{\mathrm{mmse}}$. This estimate is fed back and used to adjust the epoch of the next observation. Therefore, instead of sampling the received signal uniformly, to obtain $y_k = y(kT)$, the sampling time is adaptively selected according to the most recent estimate of the relative symbol delay, to yield $y_k = y(kT - \tilde{\tau}_k)$, where $\tilde{\tau}_k = \alpha \hat{\tau}_{k-1}^{\mathrm{mmse}}$ is the MMSE prediction of τ_k.

The observations collected in this way have the form

$$y_k = \mathrm{e}^{j(kT-\tilde{\tau}_k)\omega_k} h_k \mathbf{s}_k^\top \mathbf{g}(\tau_k - \tilde{\tau}_k) + v_k \tag{59}$$

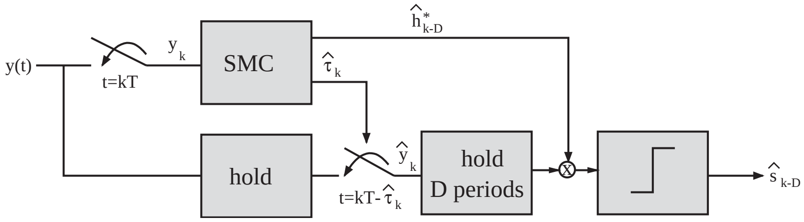

Fig. 1. Open loop architecture.

Table 1
SIS with resampling for the open-loop architecture.

Initialization
$\boldsymbol{\mu}_0 = 0$
$\boldsymbol{\Sigma}_0 = \mathbf{I}$
For $k = 0$ to M (*total no. of symbols*)
For $n = 1$ to N (*total no. of particles*)
For each $s_{k-D+L+1:k+L} \in \mathscr{S}^D$
Kalman prediction: $\{\boldsymbol{\mu}_{k-j|k-j-1}, \boldsymbol{\Sigma}_{k-j|k-j-1}\}_{j=0}^{D-1}$
Draw $\tau_k^{(n)} \sim \mathcal{N}(\alpha\tau_{k-1}^{(n)}, \sigma_u^2)$
Draw $\omega_k^{(n)} \sim \mathcal{N}(\gamma\omega_{k-1}^{(n)}, \sigma_f^2)$
Draw $s_{k-D+L}^{(n)} \sim \rho^{(n)}(s_{k-D+L})$ according to Eq. (50)
Build $\mathbf{s}_{k-D}^{(n)}$
Update weights $\tilde{w}_k^{(n)}$ according to Eq. (43)
Normalize weights $w_k^{(n)} = (\sum_{i=1}^N \tilde{w}_k^{(i)})^{-1}\tilde{w}_k^{(n)}$
Kalman update:
$\boldsymbol{\mu}_{k-D}^{(n)} = E_{p(\mathbf{h}_{k-D}|\mathbf{s}_{0:k-D}^{(n)}, \tau_{0:k-D}^{(n)}, \omega_{0:k-D}^{(n)}, y_{0:k-D})}[\mathbf{h}_{k-D}]$,
$\boldsymbol{\Sigma}_{k-D}^{(n)} = E_{p(\mathbf{h}_{k-D}|\mathbf{s}_{0:k-D}^{(n)}, \tau_{0:k-D}^{(n)}, \omega_{0:k-D}^{(n)}, y_{0:k-D})}[(\mathbf{h}_{k-D} - \boldsymbol{\mu}_{k-D})(\mathbf{h}_{k-D} - \boldsymbol{\mu}_{k-D})^H]$,
Resample if $\hat{N}_{\text{eff}} = \frac{1}{\Sigma_{n=1}^N (w_k^{(n)})^2} < N/2$
Estimate delay: $\hat{\tau}_k = \sum_{n=1}^N \tau_k^{(n)} w_k^{(n)}$
Estimate frequency offset: $\hat{\omega}_k = \sum_{n=1}^N \omega_k^{(n)} w_k^{(n)}$
Sample: $\hat{y}_k = y(t = kT - \hat{\tau}_k)$
Channel estimate: $\hat{h}_{k-D} = \sum_{n=1}^N \mathbf{c}^\top \boldsymbol{\mu}_{k-D}^{(n)} w_k^{(n)}$
Detect symbol, $\hat{s}_{k-D} = \arg\min_{s \in \mathscr{S}} \mid \hat{y}_{k-D} \mathrm{e}^{-j((k-D)T - \hat{\tau}_{k-D})\hat{\omega}_{k-D}} \hat{h}_{k-D}^* - s \mid$

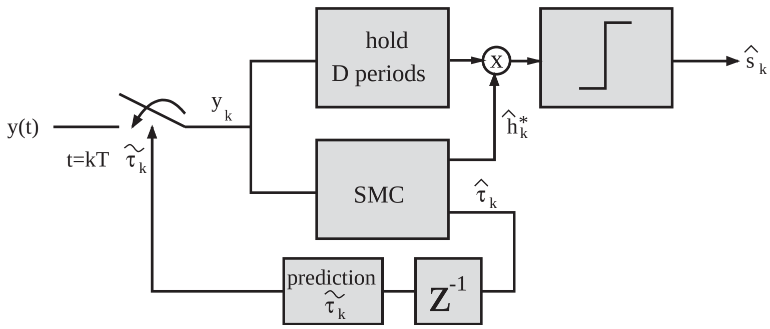

Fig. 2. Closed loop architecture.

where $h_k = h(kT - \tilde{\tau}_k)$, $\omega_k = \omega(kT - \tilde{\tau}_k)$ and the symbol vector is $\mathbf{s}_k = [s_{k-L+1}, \ldots, s_{k+L}]^\top$, if $\tau_k - \tilde{\tau}_k > 0$, and $\mathbf{s}_k = [s_{k-L}, \ldots, s_{k+L-1}]^\top$ otherwise. Notice that, if $\tilde{\tau}_k \simeq \tau_k$, the resulting observation, y_k, is free of ISI and the corresponding symbol can be optimally detected multiplying y_k by $\mathrm{e}^{-j(kT-\tilde{\tau}_k)\hat{\omega}_k^{\text{mmse}}} \hat{h}_k^*$ and using a simple threshold detector that makes a decision based on the minimal Euclidean distance between y_k and the elements in $\mathscr{S}$. As in the open-loop structure, the final detection step has to be delayed until $\hat{h}_k$ is available at time $k + D$.

The recursive steps of the proposed algorithm are summarized in Table 2.

Table 2
SIS with resampling for the closed-loop architecture.

Initialization
$\tilde{\tau}_0 = 0$
$\boldsymbol{\mu}_0 = 0$
$\boldsymbol{\Sigma}_0 = \mathbf{I}$
For $k = 0$ to M (*total number of symbols*)
Sample $y_k = y(t = kT - \tilde{\tau}_k)$
For $n = 1$ to N (*total number of particles*)
For each $s_{k-D+L+1:k+L} \in \mathscr{S}^D$
Kalman prediction: $\{\boldsymbol{\mu}_{k-j|k-j-1}, \boldsymbol{\Sigma}_{k-j|k-j-1}\}_{j=0}^{D-1}$
Draw $\tau_k^{(n)} \sim \mathcal{N}(\alpha\tau_{k-1}^{(n)}, \sigma_u^2)$
Draw $\omega_k^{(n)} \sim \mathcal{N}(\gamma\omega_{k-1}^{(n)}, \sigma_f^2)$
Draw $s_{k-D+L}^{(n)} \sim \rho^{(n)}(s_{k-D+L})$ according to Eq. (50)
Build $\mathbf{s}_{k-D}^{(n)}$
Update weights $\tilde{w}_k^{(n)}$ according to Eq. (43)
Normalize weights $w_k^{(n)} = (\sum_{i=1}^N \tilde{w}_k^{(i)})^{-1}\tilde{w}_k^{(n)}$
Kalman update: $\boldsymbol{\mu}_{k-D}^{(n)}, \boldsymbol{\Sigma}_{k-D}^{(n)}$
Resample if $\hat{N}_{\mathrm{eff}} = \frac{1}{\Sigma_{n=1}^N (w_k^{(n)})^2} < N/2$
Timing recovery, channel estimation and symbol detection
$\hat{\tau}_k = \sum_{n=1}^N \tau_k^{(n)} w_k^{(n)}$

$\hat{\omega}_k = \sum_{n=1}^N \omega_k^{(n)} w_k^{(n)}$

$\hat{h}_{k-D} = \sum_{n=1}^N \mathbf{c}^\top \boldsymbol{\mu}_{k-D}^{(n)} w_k^{(n)}$

$\hat{s}_{k-D} = \arg\min_{s\in\mathscr{S}} \mid y_{k-D}\mathrm{e}^{-j((k-D)T-\tilde{\tau}_k)\hat{\omega}_{k-D}}\hat{h}_{k-D}^* - s \mid$

Timing prediction: $\tilde{\tau}_{k+1} = \alpha\hat{\tau}_k$

5. Posterior Cramér–Rao bound

Posterior distribution estimates based on SIS algorithms converge asymptotically to the true posterior distribution as the number particles, N, approaches infinity. In practice, however, a finite number particles is used to estimate parameters of interest. As a result of this approximations a certain degradation in performance of the estimation is expected. In order to study the efficiency of the proposed estimation method, it is of great interest to compute the variance bounds on the estimation errors and compare them with the lowest bounds corresponding to the optimal estimator. In this section, we will derive a lower bound for the mean square error (MSE) in the estimation of the delay process, $\tau_{0:k}$.

When the parameter of interest is assumed fixed, the lower bound for the variance of any unbiased estimator is given by the well-known Cramér–Rao bound (CRB) [20] which, in turn, is obtained from the inverse of the Fisher information matrix (FIM). However, for Bayesian models where the parameter of interest is considered random, the lowest achievable variance is given by the PCRB [1,21]. Therefore, we wish to derive the PCRB associated to the timing process, $\tau_{0:k}$, in order to obtain a lower bound for the MSE of the delay estimates.

We define the $k+1$ dimensional vectors $\underline{\tau} = [\tau_0, \tau_1, \ldots, \tau_k]^\top$ and $\underline{\hat{\tau}} = [\hat{\tau}_0, \hat{\tau}_1, \ldots, \hat{\tau}_k]^\top$, where $\hat{\tau}_k$ is an arbitrary estimate of τ_k. For the signal model of interest in this paper, the PCRB can be stated as

$$\mathbf{P}_k = E_{p(\mathbf{s}_{0:k},\tau_{0:k},\omega_{0:k},\mathbf{h}_{0:k},y_{0:k})}\left[(\hat{\underline{\tau}} - \underline{\tau})(\hat{\underline{\tau}} - \underline{\tau})^\top\right] \geqslant \mathbf{J}(\tau_{0:k})^{-1} \tag{60}$$

where $\mathbf{J}(\tau_{0:k})$ is the $(k+1)\times(k+1)$ FIM, which is defined, element-wise, as

$$[\mathbf{J}(\tau_{0:k})]_{ij} = E_{p(\mathbf{s}_{0:k},\tau_{0:k},\omega_{0:k},\mathbf{h}_{0:k},y_{0:k})} \times \left[\frac{-\partial^2 \log\left(p(\mathbf{s}_{0:k},\tau_{0:k},\omega_{0:k},\mathbf{h}_{0:k},y_{0:k})\right)}{\partial\tau_i \partial\tau_j}\right]. \tag{61}$$

Notice that the ith element in the diagonal of $\mathbf{J}(\tau_{0:k})$, which we subsequently denote as $J_i = [\mathbf{J}(\tau_{0:k})]_{ii}$, corresponds to the inverse of the lowest achievable MSE in the estimation of τ_i.

The direct computation of the FIM is computationally prohibitive as it requires the inversion of a big matrix which grows with k. It is shown, however, in [21] that a recursive method, which sequentially evaluates the inverse of the MSE of $\hat{\tau}_{k+1}$, can be applied to compute the FIM. Specifically

$$J_{k+1} = D_k^{22} - D_k^{21}(J_k + D_k^{11})^{-1}D_k^{12}. \tag{62}$$

The terms in the above equation are

$$D_k^{11} = E_{p(\mathbf{s}_{0:k+1},\tau_{0:k+1},\omega_{0:k+1},\mathbf{h}_{0:k+1},y_{0:k+1})} \times[-\triangle_{\tau_k}^{\tau_k} \log(p(\tau_{k+1}|\tau_k))] \tag{63}$$

$$D_k^{12} = E_{p(\mathbf{s}_{0:k+1},\tau_{0:k+1},\omega_{0:k+1},\mathbf{h}_{0:k+1},y_{0:k+1})} \times[-\triangle_{\tau_k}^{\tau_{k+1}} \log(p(\tau_{k+1}|\tau_k))] \tag{64}$$

$$D_k^{21} = E_{p(\mathbf{s}_{0:k+1},\tau_{0:k+1},\omega_{0:k+1},\mathbf{h}_{0:k+1},y_{0:k+1})} \times[-\triangle_{\tau_{k+1}}^{\tau_k} \log(p(\tau_{k+1}|\tau_k))] \tag{65}$$

$$D_k^{22} = E_{p(\mathbf{s}_{0:k+1},\tau_{0:k+1},\omega_{0:k+1},\mathbf{h}_{0:k+1},y_{0:k+1})} \times[-\triangle_{\tau_{k+1}}^{\tau_{k+1}} \log(p(\tau_{k+1}|\tau_k))] \tag{66}$$

$$+ E_{p(\mathbf{s}_{0:k+1},\tau_{0:k+1},\omega_{0:k+1},\mathbf{h}_{0:k+1},y_{0:k+1})} \times[-\triangle_{\tau_{k+1}}^{\tau_{k+1}} \log\left(p(y_{k+1}|\tau_{k+1},\mathbf{s}_{k+1})\right)], \tag{67}$$

where $\triangle$ denotes the second derivative operator, defined as $\triangle_{\tau_k}^{\tau_{k+1}} = \partial^2/(\partial\tau_k\partial\tau_{k+1})$ and $\log(\cdot)$ is the natural logarithm. Recursion (62) is initialized at time $t=-1$, in the absence of observations, by considering $J_{-1} = 12/T^2$, which is the inverse of the variance of the uniform distribution in $[0,T)$. Notice that this is the only a priori information regarding the delay.

It is straightforward to numerically evaluate Eqs. (63)–(66), which yield

$$D_k^{11} = \frac{\alpha^2}{\sigma_u^2}$$

$$D_k^{12} = D_k^{21} = -\frac{\alpha}{\sigma_u^2}$$

while, as for Eq. (67),

$$D_k^{22} = \left(\frac{1}{\sigma_u^2} + E_{p(\mathbf{s}_{0:k+1},\tau_{0:k+1},\omega_{0:k+1},\mathbf{h}_{0:k+1},y_{0:k+1})} \left[\frac{1}{|\mathscr{S}|^{2L}}\sum_{\mathbf{s}_k\in\mathscr{S}^L}\frac{|\,\mathrm{e}^{jkT\omega_k}h_k|^2\left(\mathbf{s}_k^\top\nabla_{\tau_{k+1}}\mathbf{g}(\tau_{k+1})\right)^2}{\sigma_v^2}\right]\right). \tag{68}$$

Unfortunately, it is not possible to obtain a closed-form expression for the expectation in the above equation. Instead, as suggested in [21], we can estimate it using Monte Carlo simulation. When Q i.i.d. state trajectories are generated, we approximate D_k^{22} as

$$\hat{D}_k^{22} = \left(\frac{1}{\sigma_u^2} + \frac{1}{|\mathscr{S}|^{2L}Q} \times\sum_{\mathbf{s}_k\in\mathscr{S}^L}\sum_{j=1}^{Q}\frac{|\,\mathrm{e}^{jkT\omega_k}h_k|^2\left(\mathbf{s}_k^\top\nabla_{\tau_{k+1}}\mathbf{g}(\tau_{k+1}^{(j)})\right)^2}{\sigma_v^2}\right) \tag{69}$$

where $\nabla_{\tau_{k+1}} = \frac{\partial}{\partial\tau_{k+1}}$.

6. Computer simulations

Finally, we present computer simulations that illustrate the validity of our approach. We have considered a differentially encoded BPSK modulation (symbol alphabet $\mathscr{S} = \{\pm 1\}$) with symbol period of $T = 10^{-4}$ and a flat fading channel with fading rate 0.0022 (AR parameters β_1, β_2 and σ_e^2 selected accordingly). The delay has been modeled as a first-order AR process with parameter $\alpha = 0.999$ and noise variance $\sigma_u^2 = 3 \times 10^{-4}$. Similarly, the frequency error AR process is assigned parameters $\gamma = 0.999$ and noise variance of $\sigma_f^2 = 1 \times 10^{-4}$. A time-limited causal raised-cosine pulse with a roll-off factor $a = 0.9$ and an ISI spread of $2L = 4$ symbols has been used.

The performance of the proposed SMC receivers is addressed in terms of the normalized MSE attained in timing estimation and the overall SER achieved by the detectors. For comparison purposes, we have also studied the performance of classical algorithms for timing error detection and frequency offset estimation. In particular, we have studied the performance of the approximate ML timing error detector (TED) in [14, Section 7.5], the open-loop frequency estimator of [14, Section 3.4] and decision-directed Kalman filtering for estimation of the complex fading process [13]. We have combined these three standard procedures to yield a *conventional* receiver. A genie-aided version of the latter, where the frequency error is perfectly corrected and only timing error detection and Kalman filtering are performed, has also been evaluated. In both cases, detection is carried out by simple thresholding (the same as in the proposed SMC receivers).

Fig. 3 shows the normalized timing MSE attained by the proposed SMC algorithms for several values of the SNR. The normalized MSE is computed as

$$\mathrm{MSE} = \frac{1}{MQ} \sum_{k=0}^{M-1} \sum_{i=1}^{Q} \left(\frac{\tau_k - \hat{\tau}_k^{(i)}}{T} \right)^2 \tag{70}$$

where $Q = 100$ denotes the number of independent simulation trials we have carried out and $\hat{\tau}_k$ is the delay estimate. The open-loop and closed-loop SMC receivers described in Tables 1 and 2, respectively, with smoothing lag $D = 2$ and $N = 650$ particles, attain a similar MSE for the whole SNR range, which is consistently lower than the MSE of the conventional and the genie-aided receivers described above. The main reason for this performance gap is that the approximate ML TED is derived under the assumption of fixed delay ($\tau_k = \tau \ \forall k$) and low SNR and, as a consequence, it is relatively simple to implement but a clearly suboptimal algorithm.

Fig. 4 shows the variation of the MSE with time for SNR= 25 dB. We have plotted the lower bound of the MSE given the PCRB as described in Section 5. It can be seen that the proposed algorithms perform close to the optimal bound and outperform the ML TEDs.

Finally, Fig. 5 shows the SER of the SMC receivers for increasing SNR. It should be noted here that there is a delay ambiguity inherent to the blind estimation of τ_k, i.e., $\hat{\tau}_k = \tau_k$ and $\hat{\tau}_k = mT + \tau_k$, with integer m, are equally valid estimates of

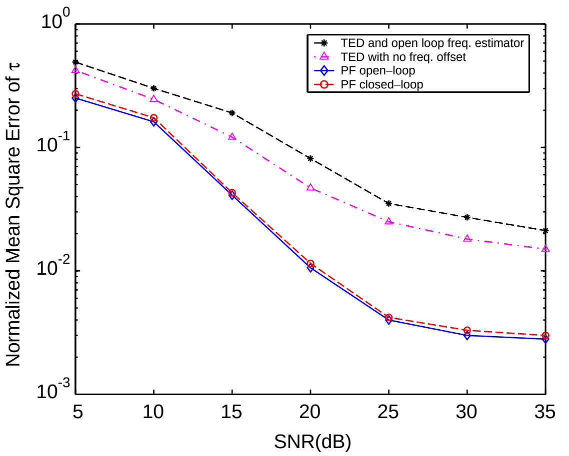

Fig. 3. MSE for several adaptive timing estimators.

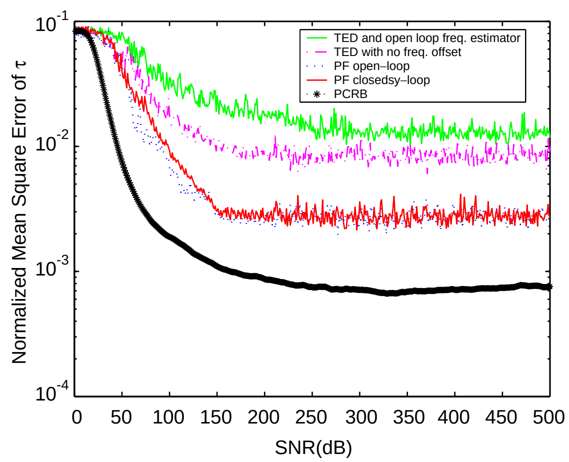

Fig. 4. MSE vs. time and PCRB for the adaptive timing estimators.

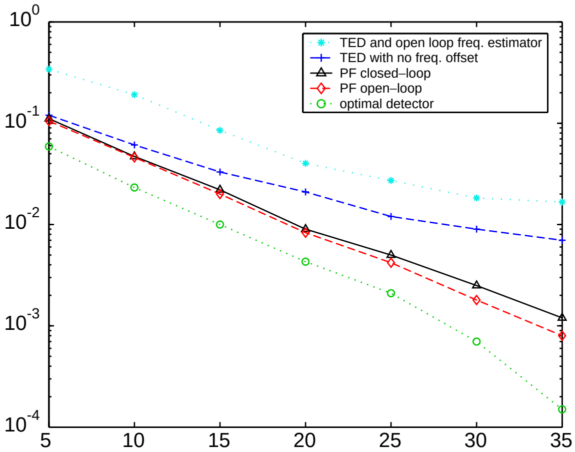

Fig. 5. SER for several detectors.

the delay, from a statistical point of view, as long as the data sequence is also delayed by m. However, this ambiguity is easily removed if the data sequence length, M, is a priori known, as assumed in this paper (and always the case in practice). It is apparent that the SER achieved by the proposed SMC adaptive receivers is very close to the optimal SER, obtained using a clairvoyant receiver with perfect knowledge of $\tau_{0:k}$, $\omega_{0:k}$, and the channel process $h_{0:k}$. The symbol error rate of the ML TED based receivers is shown to be considerably worse.

7. Conclusions

We have presented a novel algorithm for blind generalized synchronization and data detection in frequency-flat fast-fading wireless channels based on a Bayesian estimation approach and the SMC methodology. The proposed SMC technique allows to obtain asymptotically optimal estimates of the symbol time varying delays, the also time-varying frequency error and the fast fading complex channel process (which includes both amplitude attenuation and phase offset). The design of the resulting blind receiver is completed by considering suitable receiver architectures that allow the exploitation of the sequential estimation of the reference parameters in order to remove the ISI before detection and, thus, to attain close to optimal symbol error rate. The performance of the new receiver is assessed both analytically, through the posterior Crámer–Rao bound of the timing process, and numerically, through computer simulations that illustrate the superiority of the proposed detector when compared with conventional techniques based on approximate maximum likelihood timing error detection, Kalman filtering and open-loop frequency error estimation.

Acknowledgements

Joaquín Míguez ackowledges the support of *Ministerio de Ciencia y Tecnología* of Spain and Xunta de Galicia (project TIC2001-0751-C04-01). Tadesse Ghirmai, Mónica F. Bugallo and Petar M. Djurić acknowledge the support of the National Science Foundation (Award CCR-0082607).

References

[1] N. Bergman, Posterior Cramér–Rao bounds for sequential estimation, in: A. Doucet, N. deFreitas, N. Gordon (Eds.), Sequential Monte Carlo Methods in Practice, Springer, Berlin, 2001, pp. 321–338 (Chapter 15).

[2] T. Bertozzi, D.L. Ruyet, C. Panazio, H. Vu-Thien, Channel tracking using particle filtering in unresolvable multipath environments, EURASIP J. Appl. Signal Process., to appear.

[3] T. Bertozzi, D.L. Ruyet, G. Rigal, H. Vu-Thien, On particle filtering for digital communications, in: Proceedings of the IEEE Workshop on SPAWC, 2003.

[4] R. Chen, J.S. Liu, Mixture Kalman filters, J. Roy. Statist. Soc. B 62 (2000) 493–508.

[5] R. Chen, X. Wang, J.S. Liu, Adaptive joint detection and decoding in flat-fading channels via mixture kalman filtering, IEEE Trans. Inform. Theory 46 (6) (2000) 2079–2094.

[6] D. Crisan, A. Doucet, A survey of convergence results on particle filtering, IEEE Trans. Signal Process. 50(3) (2002).

[7] P.M. Djurić, J.H. Kotecha, J. Zhang, Y. Huang, T. Ghirmai, M.F. Bugallo, J. Míguez, Particle Filtering, IEEE Signal Process. Mag. 20(5) (September 2003) 19–38.

[8] A. Doucet, N. de Freitas, N. Gordon (Eds.), Sequential Monte Carlo Methods in Practice, Springer, New York, 2001.

[9] A. Doucet, N. de Freitas, N. Gordon, An introduction to sequential Monte Carlo methods, in: A. Doucet, N. de Freitas, N. Gordon (Eds.), Sequential Monte Carlo Methods in Practice, Springer, Berlin, 2001, pp. 4–14 (Chapter 1).

[10] A. Doucet, S. Godsill, C. Andrieu, On sequential Monte Carlo sampling methods for Bayesian filtering, Statist. Comput. 10 (3) (2000) 197–208.
[11] R. Iltis, Joint estimation of PN code delay and multipath using the extended Kalman filter, IEEE Trans. Comm. 38 (1990) 1677–1685.
[12] R.A. Iltis, A sequential Monte Carlo filter for joint linear/nonlinear state estimation with application to DS-CDMA, IEEE Trans. Signal Process. 51 (2003) 417–426.
[13] C. Komnikakis, C. Fragouli, A.H. Sayeed, R.D. Wesel, Multi-input multi-output fading channel tracking and equalization using kalman estimation, IEEE Trans. Signal Process. 50 (5) (2002) 1065–1076.
[14] U. Mengali, A. D'Andrea, Synchronization Techniques for Digital Receivers, Plenum Press, New York, 1997.
[15] M. Omidi, S. Pasupathy, P. Gulak, Joint data and kalman estimation for rayleigh fading channels, Wireless Personal Commun. (10) (1999) 319–339.
[16] E. Punskaya, A. Doucet, W.J. Fitzgerald, On the use and misuse of particle filtering in digital communications, in: Proceedings of EUSIPCO, 2002.
[17] E. Punskaya, A. Doucet, W.J. Fitzgerald, Particle filtering for joint symbol and parameter estimation in ds spread spectrum systems, in: Proceedings of IEEE ICASSP, 2003.
[18] E. Punskaya, A. Doucet, W.J. Fitzgerald, Particle filtering for joint symbol and code delay estimation in DS spread spectrum systems in multipath environment, in EURASIP J. Appl. Signal Process., to appear.
[19] J. Riba, J. Sala, G. Vázquez, Conditional maximum likelihood timing recovery: Estimators and bounds, IEEE Trans. Signal Process. 49 (4) (2001) 835–850.
[20] C.W. Therrien, Discrete Random Signals and Statistical Signal Processing, Prentice-Hall, Englewood Cliffs, NJ, USA, 1992.
[21] P. Tichavský, C.H. Muravchik, A. Nehorai, Posterior Cramér–Rao bounds for discrete-time nonlinear filtering, IEEE Trans. Signal Process. 46 (5) (1998) 1386–1396.
[22] G.M. Vitetta, D.P. Taylor, Maximum likelihood decoding of uncoded and coded PSK signal sequences transmitted over Rayleigh flat-fading channels, IEEE Trans. Comm. 43 (1995) 2750–2758.